

Kinetics and isothermal modeling of liquid phase adsorption of rhodamine B onto urea modified *Raphia hookerie* epicarp

A. A. Inyinbor¹ · F. A. Adekola² · G. A. Olatunji²

Received: 30 March 2016 / Accepted: 1 September 2016 / Published online: 14 September 2016
© The Author(s) 2016. This article is published with open access at Springerlink.com

Abstract Epicarp of *Raphia hookerie*, a bioresource material, was modified with urea (UMRH) to adsorb Rhodamine B (RhB) from aqueous solution. Adsorbent morphology and surface chemistry were established by Brunauer–Emmett–Teller (BET) surface area determination, Fourier transform infrared spectroscopic (FTIR) analysis, scanning electron microscopy (SEM), as well as the pH point of zero charge (pHpzc) determination. Prepared material was subsequently utilized for the uptake of Rhodamine B (RhB). Operational parameters, such as adsorbent dosage, concentration, time, and temperature, were investigated. Evidence of effective urea modification was confirmed by vivid absorption bands at 1670 and 1472 cm^{-1} corresponding to C=O and C–N stretching vibrations, respectively. Optimum adsorption was obtained at pH 3. Freundlich adsorption isotherm best fits the equilibrium adsorption data, while evidence of adsorbate–adsorbate interaction was revealed by Temkin isotherm model. The maximum monolayer adsorption capacity (q_{max}) was 434.78 mg/g. Kinetics of the adsorption process was best described by the pseudo-second-order kinetics model. Desorption efficiency was less than or equal to 25 % for all the eluents, and it follows the order $\text{HCl} > \text{H}_2\text{O} > \text{CH}_3\text{COOH}$.

Keywords *Raphia hookerie* · Biomass · Rhodamine B · Kinetics

Introduction

Rhodamine B (RhB) is a xanthenes dye characterized by high solubility in water, easy wet fastness, and fluorescence. Its unique characteristics gave it wide application potentials in dyeing of textile, paper, paint, and leathers, aside being used as a water tracer and biological stain (Li et al. 2010; Huang et al. 2016). RhB is a known carcinogen, and it causes eyes, skin, and respiratory tract irritations (Bhattacharyya et al. 2014). It increases hypothalamic cell apoptosis, as well as causes the disruption of hormonal balance (Sulistina et al. 2014). RhB laden effluents, therefore, require effective treatment before their final disposal.

Adsorption of pollutants from wastewater using activated carbon has been widely accepted due to its simplicity of operation, and ability to remove very low concentration of pollutants from wastewater (Khan et al. 2014a; Santos et al. 2015). Pyrolysis of organic materials, followed by activation via physical or chemical methods, produces activated carbon. They are characterized by large surface areas ranging between 600 and 2000 m^2/g , and very porous structure (DuyguOzsoy and Van Leeuwen 2010; Bhatnagar and Sillanpaa 2010). While activated carbon remains attractive due to the various aforementioned advantages, the economic disadvantage stemming from its raw material and processing procedure makes environmentalists seek alternatives.

Naturally occurring materials, in their raw as well as modified forms, were reported as effective adsorbents in dye removal (Khan et al. 2013, 2015; Inyinbor et al. 2016). These materials possessing low inorganic contents, high carbon contents, as well as various functional groups have high affinity for pollutants uptakes. For instance, agricultural wastes containing cellulose, hemicellulose, as well as

✉ A. A. Inyinbor
inyinbor.adejumoke@landmarkuniversity.edu.ng

¹ Department of Physical Sciences, Landmark University, Omu Aran P.M.B 1001, Nigeria

² Department of Industrial Chemistry, University of Ilorin, Ilorin P.M.B 1515, Nigeria

lignin have served as excellent materials in the adsorption of pollutants, such as heavy metals and dyes (Miretzky and Cirelli 2010). Utilizing agro wastes as low-cost adsorbent for pollution control presents economic and environmental protection advantages. Hence, materials that would have been of no value have found relevant use. While raw biomass may be utilized for the uptake of various pollutants, its efficiency may be further enhanced via modification (Khan et al. 2014b).

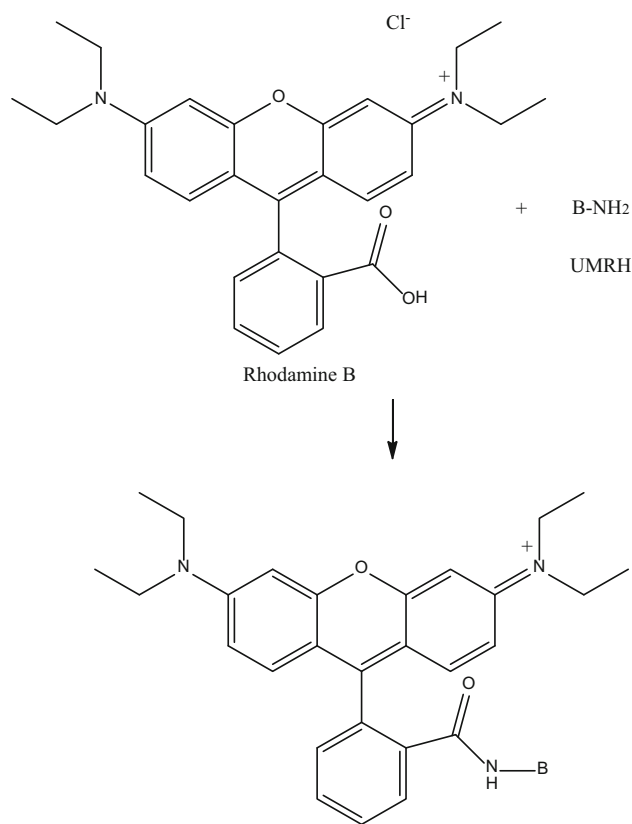
Specific functional groups in dye molecules encourage addition or substitution reactions with the $-OH$, $-SH$ or $-NH_2$ groups present in textile fibers (Rego and Ferreira 2001). Functionalization of biomaterials with chemicals containing amino groups should enhance the adsorption potential of such biomaterial, as well as present an adsorbent with specific function.

Raphia hookerie (RH) belongs to the *Palmicea* family, and has great potentials for pollutants uptake. Its neglect, viz-a-viz environmental remediation, is, therefore, a concern. We previously reported the use of raw *Raphia hookerie* (RH) fruit epicarp in the adsorption of RhB (Inyinbor et al. 2016a). This study, however, aims at enhancing the adsorption potential of RH by tailoring the surface of this readily available waste towards a specific pollutant (Rhodamine B). Currently, the epicarp of *Raphia hookerie* has no economical use, and its disposal naturally constitutes nuisance to the environment. RH was modified with urea. The approach of this treatment depends on the possibility of a reaction between the functional group(s) on RhB and $-NH_2$ (scheme 1). The prepared bioadsorbents were characterized to understand the porosity, morphology, and surface chemistry of the adsorbent. The adsorption potential in the uptake of RhB was investigated, and various adsorption operational parameters, such as effects of pH, adsorbent dosage, initial adsorbate concentration/contact time, as well as temperature, were fully reported. Kinetics, isotherm, and thermodynamics studies were employed to test the mechanism for RhB adsorption. Studies were also carried out, and reported on regeneration of the spent adsorbent.

Materials and methods

Biomass collection and pretreatment

Epicarps of *Raphia hookerie* were collected from local farmers in Makogi, Edu Local Government Area of Kwara State, Nigeria. They were washed, pulverized, and screened into particles of 150–250 μm . The pulverized RH was washed, and thereafter, dried over night in an oven controlled at 353 K.



Scheme 1 Proposed reaction between Rhodamine B and UMRH

Preparation of urea modified RH (UMRH)

To achieve urea modification, a mixture of RH and urea in a ratio of 1:2 by mass was exposed to microwave irradiation (2450 MHz) for a total period of 12 min (Farooq et al. 2010). The jelly like slurry substance obtained was boiled in water for half an hour, filtered while hot and further washed with hot water to remove unreacted urea. The residue was dried in a low-temperature oven and, thereafter, stored in an airtight container.

Adsorbent characterization

A Micrometric Tristar II surface area and porosity analyzer was employed in the BET surface area and average pore diameter determination. Samples were degassed under vacuum at 363 K for 1 h, and the temperature was further increased to 473 K overnight. Surface morphology and elemental composition were determined using a FEI/SEM Quanta 200 for SEM and EDX. Functional groups were determined with a Bruker Alpha FTIR spectrometer. The pH point of zero charge (pHpzc) was done as described in our earlier reported work (Inyinbor et al. 2015).

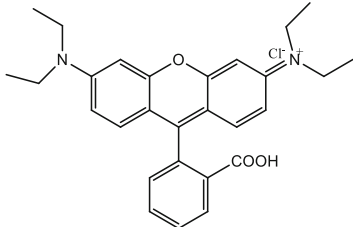
Adsorbate preparations

Rhodamine B was supplied by BDH, and its properties are as listed in Table 1. Stock solution of 1000 mg/L RhB was prepared, and the resultant working solutions of lower concentration were prepared by serial dilution of the stock solution.

Batch adsorption studies

Various adsorption operational parameters may influence adsorption process. Solution pH describes the Chemistry of particular specie in solution as well as the charge on the surface of the adsorbent. Batch adsorption studies with focus on these adsorption operational parameters, viz., initial solution pH, adsorbent dosage, initial RhB concentration, and contact time, as well as temperature on the removal of RhB, were carried out. Solution pH was varied between 2 and 10 by adding 0.1 M HCl or 0.1 M NaOH to obtain each desired pH. Adsorbent dosage was varied between 1 and 5 g/L. Varying initial RhB concentrations of 50, 100, 200, 300, and 400 mg/L was used for the effects of adsorbate concentration and contact time study. Temperature was varied between 303 and 333 K to understand the effects of temperature on RhB uptake onto UMRH. A 0.1 g UMRH was added to 100 cm³ RhB solution of a specific concentration in a 250 cm³ glass conical flask. The flask was corked and, thereafter, agitated in a temperature controlled water bath shaker, operated at 130 rpm; for a pre-determined time. Separation of unadsorbed dye and spent adsorbent was done by centrifugation, while concentration of unadsorbed dye was determined using a Beckman Coulter Du 730 UV/Vis spectrophotometer, operated at 554 nm.

Table 1 Properties of Rhodamine B

Parameters	Values
Suggested name	Rhodamine B
C.I number	45170
C.I name	Basic violet 10
Class	Rhodamine
λ_{\max}	554nm
Molecular formular	C ₂₈ H ₃₁ N ₂ O ₃ Cl
Molecular weight	479.02
Chemical structure	

Quantity of RhB adsorbed and percentage RhB removal

Quantity adsorbed at a given time t was calculated using Eq. 1, and percentage removal was obtained using:

$$q_t = \frac{(C_i - C_t) \times V}{M} \quad (1)$$

$$\% \text{Removal} = \frac{(C_i - C_f)}{C_i} \times 100, \quad (2)$$

where C_i , C_t , and C_f are the initial concentration, the concentration of RhB at time t , and final concentration of RhB, respectively. V is the volume of RhB solution used for the adsorption studies in liter, and M is the weight of the adsorbent in g.

Mathematical modeling

Isothermal studies

Equilibrium adsorption data were analyzed using the Langmuir, Freundlich, Temkin, and Dubinin–Radushkevich (D–R) adsorption isotherm models. The Langmuir isotherm (Langmuir 1916) assumes a surface with homogeneous binding sites, while the Freundlich isotherm (Freundlich 1906) describes multilayer adsorption. Temkin isotherm (Temkin and Pyzhev 1940) assumes linear rather than logarithm decrease in heat of adsorption, while ignoring extremely low and very high concentration. Last, Dubinin Radushkevich (D–R) model (Dubinin and Radushkevich 1947) gives insight into the biomass porosity, as well as the adsorption energy. These isotherms are expressed by Eqs. 3–6, respectively. The dimensionless equilibrium parameters (R_L), which explains the favorability of adsorption, Polanyi potential (ε), and the mean energy of adsorption (E), can be obtained by Eqs. 3a, 6a, and 6b, respectively:

$$\frac{C_e}{q_e} = \frac{C_e}{q_{\max}} + \frac{1}{q_{\max} K_L} \quad (3)$$

$$R_L = \frac{1}{(1 + K_L C_o)} \quad (3a)$$

$$\log q_e = \frac{1}{n} \log C_e + \log K_f \quad (4)$$

$$q_e = B \ln A + B \ln C_e \quad (5)$$

$$\ln q_e = \ln q_o - \beta \varepsilon^2 \quad (6)$$

$$\varepsilon = RT \ln \left(1 + \frac{1}{C_e} \right) \quad (6a)$$

$$E = \sqrt{\frac{1}{2\beta}}, \quad (6b)$$

where C_e is the equilibrium concentration of RhB dye (mg/L), q_e is the quantity of RhB dye adsorbed onto the adsorbent at equilibrium (mg/g), q_{\max} is the maximum monolayer adsorption capacity of adsorbent (mg/g), and K_L is the Langmuir adsorption constant (L/mg). K_f and n are Freundlich constants incorporating the factors affecting the adsorption capacity and adsorption intensity, respectively. A is the Temkin isotherm constant (L/g), from the value of Temkin constant B , b (J/mol) which is a constant related to the heat of absorption can be obtained from the expression $B = RT/b$, T is the absolute temperature (K), and R is the gas constant (8.314 J/mol/K). The value of adsorption energy (E) obtained from the D–R model further provides information as to whether adsorption process is physical or chemical in nature, β which is the activity coefficient helps in obtaining the mean sorption energy E (kJ/mol).

Kinetics model

The kinetic of the adsorption systems were studied using the pseudo-first-order, pseudo-second-order, Elovich, and Avrami kinetics models. The intraparticle diffusion model was used to investigate the mechanism of adsorption process. Equations 7–11 are the linear forms of the pseudo-first-order kinetic model of Lagergren (Lagergren and Svenska 1898), pseudo-second-order kinetic model (Ho and McKay 1999), Elovich (Aharoni and Ungarish 1976), Avrami (Avrami 1940) and the intraparticle diffusion model by Weber and Morris (Weber and Morris 1963), respectively:

$$\ln(q_e - q_t) = \ln q_e - k_1 t \quad (7)$$

$$\frac{t}{q_t} = \frac{1}{k_2 q_e^2} + \frac{t}{q_e} \quad (8)$$

$$q_t = \frac{1}{\beta} \ln(\alpha\beta) + \frac{1}{\beta} \ln t \quad (9)$$

$$\ln[-\ln(1 - \alpha)] = n_{AV} K_{AV} + n_{AV} \ln t \quad (10)$$

$$q_t = k_{\text{diff}} t^{1/2} + C, \quad (11)$$

where q_e is the quantity adsorbed at equilibrium (mg/g) and q_t is the quantity adsorbed at time t (mg/g). α is a constant related to chemisorption rate and β is a constant which depicts the extent of surface coverage. K_{AV} is the Avrami constant and n_{AV} is the Avrami model exponent of time related to the change in mechanism of adsorption. k_1 , k_2 , and k_{diff} are the rate constant for the pseudo-first-order sorption min^{-1} , the rate constant of the pseudo-second-order kinetic g/mg min^{-1} , and the rate constant for intraparticle diffusion ($\text{mg g}^{-1} \text{min}^{-1/2}$), respectively. Insight into the thickness of the boundary layer can be obtained from the value of C . Large intercept suggests great boundary layer effect.

Validation of adsorption kinetics

Sum square of error (SSE), Chi-square (X^2), and the normalized standard deviation ($\Delta q_e(\%)$), represented by Eqs. 12–14, were used to validate the kinetics model:

$$\text{SSE} = \sum_{i=1}^n (q_{\text{cal}} - q_{\text{exp}})^2 \quad (12)$$

$$X^2 = \sum_{i=1}^n \frac{(q_{\text{exp}} - q_{\text{cal}})^2}{q_{\text{cal}}} \quad (13)$$

$$\Delta q_e(\%) = 100 \sqrt{\left[\frac{(q_{\text{exp}} - q_{\text{cal}})/q_{\text{exp}}}{N - 1} \right]}. \quad (14)$$

Thermodynamic studies

Thermodynamic parameters that explain feasibility, spontaneity, and the nature of adsorbate–adsorbent interactions (ΔG° , ΔH° , and ΔS°) were calculated using the mathematical relations:

$$\ln K_o = \frac{\Delta S^\circ}{R} - \frac{\Delta H^\circ}{RT} \quad (15)$$

$$\Delta G^\circ = -RT \ln K_o, \quad (16)$$

where T is the temperature in Kelvin, R is the gas constant, and K_o can be obtained from q_e/C_e . ΔH° and ΔS° can be obtained from the plot of $\ln K_o$ versus $1/T$.

Spent adsorbent regeneration studies

To ascertain regeneration and reuse of UMRH, leaching/desorption of RhB from UMRH surface was investigated using deionized water, 0.1 M HCl and 0.1 M CH_3COOH . A 0.1 g of fresh adsorbent was loaded with RhB by agitating mixture of 0.1 g and 100 cm^3 of 100 mg/L RhB solution at pH 3.0 for 1 h. The RhB-loaded adsorbent was separated by centrifugation and the residual RhB concentration determined spectrophotometrically. To remove the unadsorbed dye, the RhB loaded adsorbent was gently washed with water, and dried. The desorption process was carried out by mixing 100 cm^3 of each desorbing eluent with the dried loaded-adsorbent and shaken for a predetermined time, and the desorbed RhB was determined spectrophotometrically. Desorption efficiency was calculated using the mathematical relation:

$$\text{Desorption efficiency (\%)} = \frac{q_{\text{de}}}{q_{\text{ad}}} \times 100, \quad (17)$$

where q_{de} is the quantity desorbed by each of the eluent, and q_{ad} is the adsorbed quantity during loading.

Results and discussion

Characterization of UMRH

The BET surface area of UMRH was very low. This is a characteristic of lignocellulosic materials (Omorogie et al. 2012; Zhang et al. 2013; Inyinbor et al. 2015a). BET surface area determination of agro waste is usually difficult as the lignocellulosic materials are burnt before degassing temperature is attained. Reducing the degassing temperature subsequently results into the presence of moisture, thus low surface area of the material. The carbon content of UMRH was found to be high (Table 2), thereby making it a suitable material for the uptake of organic pollutants (Wang et al. 2011).

FTIR spectral of RH and UMRH is shown in Fig. 1. For RH, absorption bands were observed at 1029, 1424, and 3297 cm^{-1} corresponding to C–OH stretching vibrations, CH_3 bending vibrations, and O–H of alcohol, respectively. The absorption band for methylene vibrations occurred at 2934 cm^{-1} in RH. However, great reduction in the intensities of methylene, C–OH, and O–H vibrations was observed in FTIR spectrum of UMRH. Removal of adventitious water, elimination of volatile compounds, as well as breakdown of hemicellulose may account for such reduction in intensity. New peaks were observed at 1670 and 1472 cm^{-1} . These peaks correspond with C=O and C–N stretching vibrations, respectively. The two functional groups present in urea are the carbonyl and the amino groups. Vivid appearance of these functional groups in UMRH shows that RH was successfully modified with urea. The new peak at 1472 cm^{-1} may also indicate that the peak at 3355 cm^{-1} is a characteristic of absorption band of N–H stretching vibrations (Stuart 2004).

Table 2 Characteristics of UMRH

Parameters	Values UMRH
pH	6.18
pHpzc	7.60
Bulk density	0.28
Moisture content (%)	8.13
Ash content (%)	3.53
BET surface area (m^2/g)	<0.001
Elemental composition (%)	
Carbon	70.88
Oxygen	28.68
Potassium	0.31

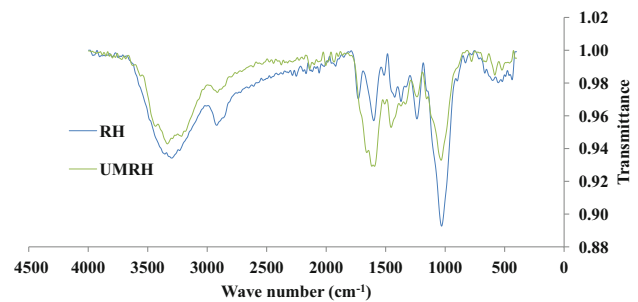


Fig. 1 FTIR spectral of RH and UMRH

Figure 2a and b shows the SEM micrograph of RH and UMRH. Numerous cavities exist on the surface of RH. Microwave irradiation and urea treatment effect, however, left numerous pores on the walls of the cavities. A deep mesopore was also created in the middle of UMRH. Texture of the adsorbent may have been altered by microwave irradiation (Foo and Hameed 2009). Hollows, pores, and cavities are important in solid–liquid adsorption, serving as transport paths for adsorbate movement (Wang et al. 2015). However, after RhB uptake, the smooth surfaces of the adsorbents were observed to be rough, and the visible openings scarcely exist (Fig. 2c).

Adsorption of rhodamine B (RhB) onto UMRH

Effects of initial adsorbate pH

The pH effect is highly important in adsorption studies. The existence of adsorbate in solution, as well as the charge on the adsorbent surface, greatly depends on solution pH. Percentage adsorption increased drastically, as adsorbate solution pH increased from 2 to 3. The pHpzc of the adsorbent was in the neutral media with value 7.60. At low pH, adsorbent surface is positively charged, and thus, repulsion between the positive adsorbent surface and cationic form of RhB may result in low adsorption. However, as the pH increased, the number of positive charge on the adsorbent reduces; hence, percentage adsorption also increases. This phenomenon was obeyed between pH of 2 and 3. Maximum adsorption of 86.79 % was obtained at pH 3 (Fig. 3). Highest adsorption of RhB onto the adsorbents at pH 3 may be as a result of diverse existence of RhB in different solution media. RhB exists as cationic (RhB^+) at pH between 1 and 3, lactonic (RhBH^{2+}) at pH of less than 1.0, and zwitterionic (RhB^\pm) at pH greater than 3.7. The zwitterionic form of RhB which occurs at $\text{pH} > 3.7$ has the tendency of dimerization, due to attractions between the carboxyl and xanthenes groups of RhB monomers. Hence,

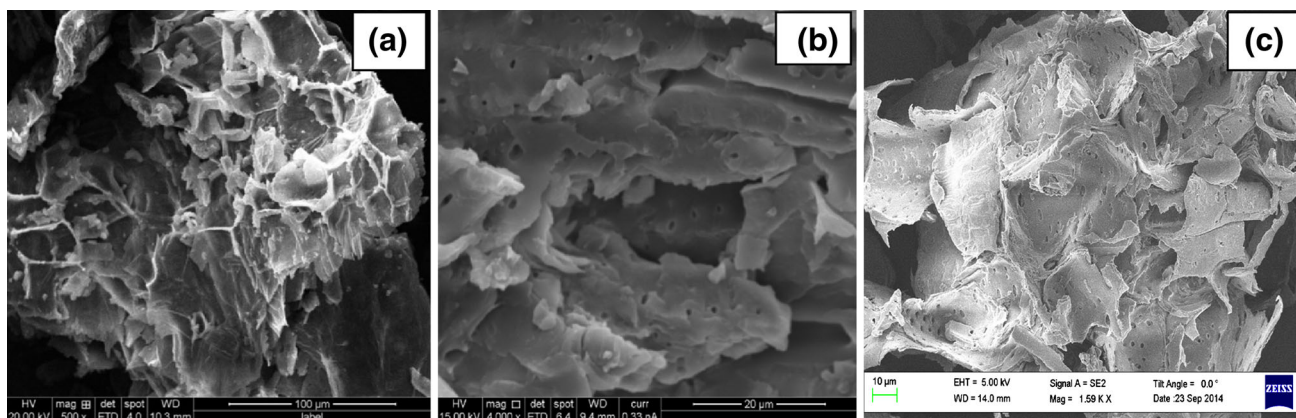


Fig. 2 SEM micrograph of RH (a) UMRH before RhB uptake and (b) after RhB uptake (c)

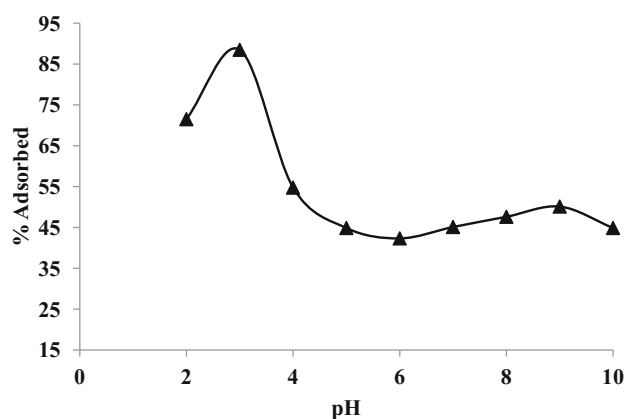


Fig. 3 Effects of pH on RhB adsorption onto UMRH. [dosage (1 g/L), agitation speed (130 rpm), agitation time (60 min), temperature (26 °C), initial adsorbate concentration (100 mg/L)]

absorption of RhB becomes difficult, resulting into decrease in adsorbent adsorption capacity. Maximum adsorption of RhB at pH 3 has been previously reported by researchers (Inyinbor et al. 2014; Ma et al. 2016; Huang et al. 2016). Subsequent adsorption studies were carried out at optimum pH (pH of 3).

Effects of adsorbent dosage

The effect of adsorbent dosage was carried at a fixed concentration of 100 mg/L and temperature of 299 K while varying the adsorbent dosage between 1 and 5 g/L. There was a rapid increase in percentage RhB removal from 84.96 to 92.48 %, as the adsorbent dosage increased from 1 to 2 g/L (Fig. 4). However, no further increase in percentage adsorption was observed after 2 g/L dosage, thereby leading to the attainment of equilibrium (Fig. 4). Increase in available adsorption sites as adsorbent dosage increased may have led to increase in percentage RhB removal (Angin 2014). However,

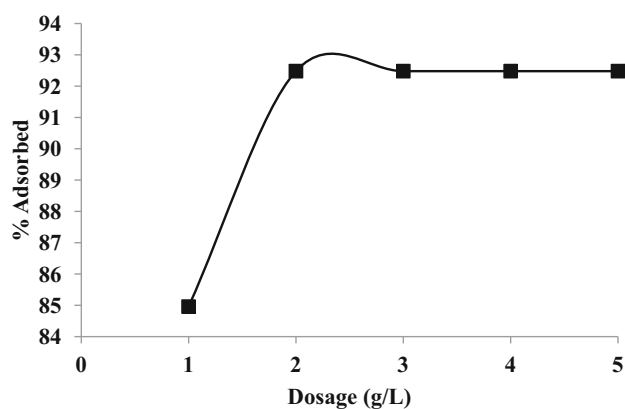


Fig. 4 Effects of adsorbent dosage on RhB adsorption onto UMRH [agitation speed (130 rpm), initial concentration (100 mg/L), temperature (26 °C), pH (3)]

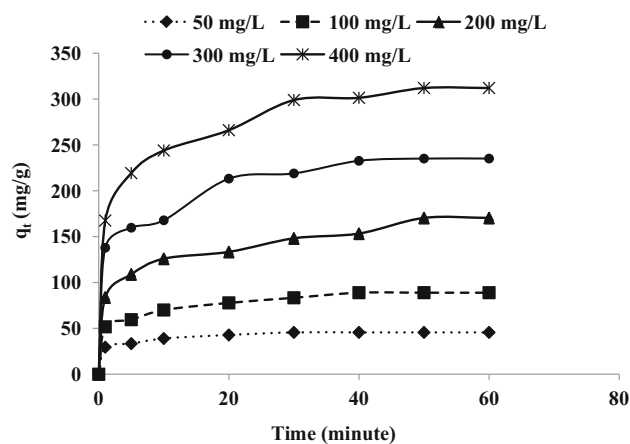


Fig. 5 Effects of concentration/contact time on RhB adsorption onto UMRH [conditions: dosage = 0.1 g, temperature = 26 °C and agitation speed = 130 rpm]

saturation of adsorption site and agglomeration resulted into no further adsorption at higher adsorbent dosage (Pirbazari et al. 2014).

Effects of contact time and adsorption kinetics

Quantity of RhB adsorbed increased with time and concentration. Increase in concentration is known to provide an increase in driving force to overcome mass transfer resistance of RhB between the aqueous and solid phases. Adsorption kinetics were fast, and equilibrium was attained after 40 min (Fig. 5). Quantities adsorbed at equilibrium for various concentrations considered, are listed on Table 3.

For the pseudo-second-order kinetic, there was close agreement between the calculated quantity adsorbed at

equilibrium (q_{cal}), and experimentally determined quantity adsorbed at equilibrium (q_{exp}), across the initial RhB concentrations considered (Table 3). High correlation coefficient ($R^2 > 0.99$) recorded for the pseudo-second-order kinetics viz-a-viz low values of X^2 , SSE and $\Delta q(\%)$ suggests a good fitting of adsorption data into this kinetic model. Adsorption data also fitted well into Elovich kinetic models, as X^2 , SSE and $\Delta q(\%)$ were also found to be generally low. Kinetic data fits into the kinetics models in this order: Pseudo-second order > Elovich > Pseudo-first order > Avrami models. A single linear profile was obtained for the intraparticle diffusion plot of UMRH-RhB

Table 3 List of parameters obtained from the pseudo-first-order, pseudo-second-order, Elovich, Avrami, and intraparticle diffusion kinetic model parameters for the adsorption of RhB onto UMRH

Constants	UMRH				
	50	100	200	300	400
q_e experimental (mg/g)	45.56	88.9	170.37	235.14	312.11
Pseudo-first order					
q_e calculated (mg/g)	15.62	47.39	77.69	130.63	142.71
$K_1 \times 10^{-2}$ (min ⁻¹)	7.82	8.57	3.96	8.83	6.85
R^2	0.9501	0.9476	0.9673	0.9354	0.9637
SSE	896.40	1723.08	8589.58	10922.34	28696.36
X^2	57.389	36.36	110.56	83.61	201.08
Δq_e (%)	30.64	25.83	27.88	25.19	27.85
Pseudo-second order					
q_e calculated (mg/g)	46.95	92.59	175.44	243.9	322.58
$K_2 \times 10^{-3}$ (g mg ⁻¹ min ⁻¹)	14.40	4.26	1.49	1.50	1.22
R^2	0.9993	0.9979	0.9908	0.9973	0.9979
SSE	1.93	13.62	25.71	76.74	109.62
X^2	0.04	0.15	0.15	0.32	0.34
Δq_e (%)	6.60	7.70	6.52	7.29	6.92
Elovich					
α_{E1} (mg/g.min)	2713.05	1159.89	843.77	2913.76	3008.97
β_{E1} (g/mg)	0.22	0.09	0.05	0.04	0.03
R^2	0.9550	0.9631	0.9622	0.9288	0.9874
SSE	1.61	0.77	25.40	1.21	8.70
X^2	0.03	0.01	0.15	0.01	0.03
Δq_e (%)	6.31	3.76	6.50	2.59	3.68
Avrami					
n_{Av}	0.32	0.33	0.33	0.41	0.40
K_{av} (min ⁻¹)	0.84	0.46	0.26	0.41	0.39
R^2	0.8947	0.9172	0.9741	0.8201	0.9345
SSE	1963.38	7707.08	28723.47	54667.12	96621.51
X^2	1570.70	6943.32	32273.56	41103.09	76079.93
Δq_e (%)	37.27	37.56	37.69	37.68	37.72
Intraparticle diffusion					
$C \times 10^2$ (mg g ⁻¹)	0.13	0.26	0.52	0.99	1.33
K_{diff} (mg g ⁻¹ min ^{-1/2})	2.27	5.86	11.41	15.11	21.43
R^2	0.8509	0.9488	0.9590	0.9412	0.9455

system and R^2 value ranged between 0.8509 and 0.9590. β_{EI} which describe the extent of surface coverage was found to decrease with increase in concentration. This further indicates that adsorption process may be described by Elovich model. While boundary layer thickness increased with increase in initial RhB concentration, intraparticle diffusion rate also behaved in a similar manner. High concentration gradient is generated via increase in initial concentration, thus faster diffusion and quick uptake of adsorbate. The plot of q_t versus $t^{1/2}$, however, did not pass through the origin, and thus, intraparticle diffusion is not the rate limiting step.

Equilibrium data and isothermal studies

The values of R_L and n were found to be less than 1 and greater than 1, respectively, for the adsorption system. This suggests favorable adsorption process. Freundlich adsorption isotherm best describes the uptake of RhB onto UMRH, suggesting that adsorption of RhB was not onto a uniform site. A very good correlation coefficient was recorded for the Langmuir, Freundlich, and Temkin adsorption isotherms. The rapid initial adsorption that characterized the RhB uptake may have followed the Langmuir adsorption type in which RhB removal was based on its interactions with the surface functional groups. Pore penetration, and adsorbate–adsorbate interaction must have resulted to the later gradual RhB uptake before equilibrium was finally attained. Adsorbate was held to non-uniform sites, and thus, Freundlich isotherm was followed. Temkin isotherm ($R^2 = 0.9500$) further validates the occurrence of adsorbate–adsorbate interactions (Bhattacharyya et al. 2014). Judging from the R^2 values, equilibrium adsorption data fit into isothermal models in this order: Freundlich > Langmuir > Temkin > Dubinin–Radushkevich. The maximum monolayer adsorption capacity obtained are reported in Table 4, and compared with other previously reported literatures (Table 5). Energy of adsorption as obtained from the D–R model suggests that chemisorption dominates the uptake of RhB onto UMRH.

Effects of temperature and thermodynamics studies

Increase in temperature results into activation of more adsorption sites in UMRH, thus resulting into increase in adsorption efficiency of the adsorbents at high temperature. Positive enthalpy (ΔH°) recorded for UMRH–RhB systems suggests that the adsorption process was endothermic in nature (Table 6). ΔS° value for UMRH–RhB systems was positive, thereby suggesting that there was increase in the randomness at the solid–liquid interface during the adsorption of RhB onto UMRH. The randomness at the solid–liquid interface could result from the higher

Table 4 Isotherm constants for the adsorption of RhB onto UMRH

Isotherms	Constants	UMRH
Langmuir	q_{max} (mg/g)	434.78
	K_L (L mg ⁻¹)	0.023
	R_L	0.0972
	R^2	0.9540
Freundlich	K_F	18.94
	n	1.60
	R^2	0.9923
Temkin	B	84.72
	A (L/g)	0.31
	b (J/mol)	29.44
	R^2	0.9500
D–R	q_o (mg/g)	204.04
	β (mol ² kJ ⁻²)	0.0063
	E (kJ mol ⁻¹)	8.91
	R^2	0.7800

Table 5 Comparison of the maximum monolayer adsorption capacity (q_{max}) of RhB onto UMRH with others reported in the literature

Adsorbent	q_{max} (mg/g)	References
Activated pyrolytic tire char	307.20	Li et al. 2010
Modified ternary waste	213.00	Anandkumar and Mandal 2011
Kaolinite	46.08	Khan et al. 2012
Fe- supported bentonite	227.25	Gao et al. 2015
Modified dika nut	526.32	Inyinbor et al. 2015a
Carbon residue activated carbon	189.83	Maneerung et al. 2016
Fe-montmorillonite	258.76	Ma et al. 2016
Lythrum sahcaria activated carbon (LSAC)	370.37	Huang et al. 2016
Modified LSAC	384.62	Huang et al. 2016
Urea modified Raphia hookerie	434.78	This study

translational entropy acquired by the displaced water molecules, as compared to that lost as a result of dye uptake (Mittal and Mishra 2014). ΔG° values obtained were negative (Table 6), suggesting spontaneity of adsorption process. Higher negative values at higher temperature suggest that adsorption process at higher temperature was more spontaneous.

Desorption studies

Several contacts points between dye molecules and adsorbents usually results into large net adsorption energy, and subsequently low desorption (Fernandez and G.V., Nunell, P.R. Bonelli, and A.L. Cukierman, 2010). In this study, desorption efficiencies of the three eluents were low

Table 6 Thermodynamic parameters for the uptake of RhB onto UMRH

Adsorbents	ΔH°	ΔS°	ΔG°				
	(kJ/mol)	(J/mol/ K)	(kJ/mol)	303	313	323	333
UMRH	42.37	143.44	-1.19	-2.32	-4.08	-5.39	

(generally less than 40 %). This suggests that RhB was held fast on the surface of the adsorbent. Desorption efficiency follows the order $\text{HCl} > \text{H}_2\text{O} > \text{CH}_3\text{COOH}$, and it was obtained to be 25, 12.50, and 10.42 % for HCl, H_2O , and CH_3COOH , respectively.

Conclusion

Prepared adsorbent was found to be effective in the uptake of RhB. Optimum adsorption was obtained at pH 3, RhB percentage removal rose up 92.48 % for adsorbent dosage of 2 g/L. Multilayer adsorption was vivid for all the adsorption systems, and thus, Freundlich isotherm best describes the adsorption of RhB onto the adsorbent. However, surface coverage as well as adsorbate–adsorbate interactions also played a predominant role in RhB uptake onto UMRH. Maximum monolayer adsorption capacity was 434.78 mg/g. Pseudo-second-order kinetics and Elovich model best described the adsorption process, and the adsorption process was spontaneous, feasible, and endothermic.

Acknowledgments The authors gratefully acknowledge the efforts of Miss Fola Funke Oyinloye for the language editing of our manuscript.

Open Access This article is distributed under the terms of the Creative Commons Attribution 4.0 International License (<http://creativecommons.org/licenses/by/4.0/>), which permits unrestricted use, distribution, and reproduction in any medium, provided you give appropriate credit to the original author(s) and the source, provide a link to the Creative Commons license, and indicate if changes were made.

References

- Aharoni C, Ungarish M (1976) Kinetics of activated chemisorptions. Part I: the non-Elovichian part of the isotherm. *J Chem Soc Faraday Trans* 72:265–268
- Anandkumar J, Mandal B (2011) Adsorption of Chromium (VI) and Rhodamine B by surface modified tannery waste: kinetics, mechanics and thermodynamics. *J Hazard Mater* 186(2–3):1088–1096
- Angin D (2014) Utilization of activated carbon produced from fruit juice industry solid waste for the adsorption of Yellow 18 from aqueous solutions. *Bioresour Technol* 168:259–266

- Avrami M (1940) Kinetics of phase change: transformation-time relations for random distribution of nuclei. *J Chem Phys* 8:212–224
- Bhatnagar A, Sillanpaa M (2010) Utilization of agro-industrial and municipal waste materials as potential adsorbents for water treatment—A review. *Chem Eng J* 157:277–296
- Bhattacharyya KG, SenGupta S, Sarma GK (2014) Interactions of the dye, Rhodamine B with kaolinite and montmorillonite in water. *Appl Clay Sci* 99:7–17
- Dubinin MM, Radushkevich LV (1947) Equation of the characteristic curve of activated charcoal. *Proc Acad Sci Phys Chem USSR* 55:331–333
- DuyguOzsoy H, Van Leeuwen J (2010) Removal of color from fruit candy waste by activated carbon adsorption. *J Food Eng* 101:106–112
- Farooq U, Khan MA, Athar M, Sakina M, Ahmad M (2010) Environmentally benign urea-modified triticum aestivum biomass for lead (II) elimination from aqueous solutions. *Clean-Soil Water Air* 38(1):49–56
- Fernandez ME, Nunell GV, Bonelli PR, Cukierman AL (2010) Effectiveness of Cupressus sempervirens cones as biosorbent for the removal of basic dyes from aqueous solutions in batch and dynamic modes. *Bioresour Technol* 101:9500–9507
- Foo KY, Hameed BH (2009) Recent developments in the preparation and regeneration of activated carbons by microwaves. *Adv Colloid Interface Sci* 149:19–27
- Freundlich HMF (1906) Over the adsorption in solution. *Z Phys Chem* 57:385–470
- Gao Y, Wang Y, Zhang H (2015) Removal of Rhodamine B with Fe-supported bentonite as heterogeneous photo-Fenton catalyst under visible irradiation. *Appl Catal B* 178:29–36
- Ho YS, McKay G (1999) Pseudo-second order model for sorption processes. *Process Biochem* 34:451–465
- Huang Y, Zheng X, Feng S, Guo Z, Liang S (2016) Enhancement of rhodamine B removal by modifying activated carbon developed from *Lythrum salicaria* L. with pyruvic acid. *Colloids Surf A physicochem Eng Asp* 489:154–162
- Inyinbor AA, Adekola FA, Olatunji GA (2014) Adsorption of Rhodamine B from aqueous effluent using treated epicarp of *Raphia hookerie*. *Covenant Univ J Phys Life Sci (CJPL)* 2(2):83–101
- Inyinbor AA, Adekola FA, Olatunji GA (2015a) Adsorption of rhodamine B dye from aqueous solution on *Irvingia gabonensis* biomass: kinetics and thermodynamics studies. *S Afr J Chem* 68:115–125
- Inyinbor AA, Adekola FA, Olatunji GA (2015b) EDTA modified *Irvingia gabonensis*: an efficient bioresource material for the removal of Rhodamine B. *Pak J Anal Environ Chem* 16(2):38–45
- Inyinbor AA, Adekola FA, Olatunji GA (2016) Liquid phase adsorptions of Rhodamine B dye onto raw and chitosan supported mesoporous adsorbents: isotherms and kinetics studies. *Appl Water Sci* 1–11. doi:10.1007/s13201-016-0405-4, <http://link.springer.com/article/10.1007/s13201-016-0405-4>
- Inyinbor AA, Adekola FA, Olatunji GA (2016b) Kinetic and thermodynamic modeling of liquid phase adsorption of Rhodamine B dye onto *Raphia hookerie* fruit epicarp. *Water Resour Ind* 15:14–27
- Khan TA, Dahiya S, Ali I (2012) Use of kaolinite as adsorbent: equilibrium, dynamics and thermodynamic studies on the adsorption of Rhodamine B from aqueous solution. *Appl Clay Sci* 69:58–66
- Khan TA, Nazir M, Khan EA (2013) Adsorptive removal of rhodamine B from textile wastewater using water chestnut (*Trapa natans* L.) peel: adsorption dynamics and kinetic studies. *Toxicol Environ Chem* 95(6):919–931

- Khan TA, Sharma S, Khan EA, Mukhlif AA (2014a) Removal of congo red and basic violet 1 by chir pine (*Pinus roxburghii*) sawdust, a saw mill waste: batch and column studies. *Toxicol Environ Chem* 96(4):555–568
- Khan TA, Rahman R, Ali I, Khan EA, Mukhlif AA (2014b) Removal of malachite green from aqueous solution using waste pea shells as low-cost adsorbent adsorption isotherms and dynamics. *Toxicol Environ Chem*. doi:10.1080/02772248.2014.969268
- Khan TA, Khan EA, Shahjahan (2015) Removal of basic dyes from aqueous solution by adsorption onto binary iron-manganese oxide coated kaolinite: non-linear isotherm and kinetics modeling. *Appl Clay Sci* 107:70–77
- Lagergren S, Svenska BK (1898) On the theory of so-called adsorption of materials. *R. Swed Acad Sci Doc* 24:1–13
- Langmuir I (1916) The constitutional and fundamental properties of solids and liquids. *J Am Chem Soc* 38:2221–2295
- Li L, Liu S, Zhu T (2010) Application of activated carbon derived from scrap tires for adsorption of Rhodamine B. *J Environ Sci* 22(8):1273–1280
- Ma L, Xi Y, He H, Ayoko GA, Zhu R, Zhu J (2016) Efficiency of Fe-montmorillonite on the removal of Rhodamine B and hexavalent chromium from aqueous solution. *Appl Clay Sci* 120:9–15
- Maneerung T, Liew J, Dai Y, Kawi S, Chong C, Wang C (2016) Activated carbon derived from carbon residue from biomass gasification and its application for dye adsorption: kinetics, isotherms and thermodynamic studies. *Bioresour Technol* 200:350–359
- Miretzky P, Cirelli AF (2010) Cr(VI) and Cr(III) removal from aqueous solution by raw and modified lignocellulosic materials: a review. *J Hazard Mater* 180:1–19
- Mittal H, Mishra SB (2014) Gum ghatti and Fe₃O₄ magnetic nanoparticles based nanocomposites for the effective adsorption of rhodamine B. *Carbohydr Polym* 101:1255–1264
- Omorogie MO, Babalola JO, Unuabonah EI, Song W, Gong JR (2012) Efficient chromium abstraction from aqueous solution using a low-cost biosorbent: *nauclea diderrichii* seed biomass waste. *J Saudi Chem Soc*. doi:10.1016/j.jscs.2012.09.017
- Pirbazari AE, Saberikhah E, HabibzadehKozani SS (2014) Fe₃O₄-wheat straw: preparation, characterization and its application for methylene blue adsorption. *Water Resour Ind* 7–8:23–37
- Rego B, Ferreira V (2001) Combined studies involving photonic and electronic spectroscopies. *Adv surf Sci* 38:327
- Santos S, Ungureanu G, Boaventura R, Botelho C (2015) Selenium contaminated waters: an overview of analytical methods, treatment options and recent advances in sorption methods. *Sci Total Environ* 521–522:246–260
- Stuart B (2004) *Infrared spectroscopy: fundamentals and applications*. Wiley, New Jersey. ISBNs: 0-470-85427-8 (HB); 0-470-85428-6 (PB)
- Sulistina DR, Ratnawati R, Wiyasa IA (2014) Rhodamine B increases hypothalamic cell apoptosis and disrupts hormonal balance in rats. *Asian Pac J Reprod* 3(3):180–183
- Temkin MI, Pyzhev V (1940) Kinetics of ammonia synthesis on promoted iron catalyst. *Acta Physicochimica USSR* 12:327–356
- Wang XJ, Wang Y, Wang X, Liu M, Xia SQ, Yin DQ, Zhang YL, Zhao JF (2011) Microwave-assisted preparation of bamboo charcoal-based iron containing adsorbents for Cr(VI) removal. *Chem Eng J* 174:326–332
- Wang G, Zhang S, Yao P, Chen Y, Xu X, Li T, Gong G (2015) Removal of Pb(II) from aqueous solutions by *Phytolacca americana* L. biomass as a low cost biosorbent. *Arab J Chem*. doi:10.1016/j.arabjc.2015.06.011
- Weber WJ, Morris JC (1963) Kinetics of adsorption on carbon from solution. *J Sanit Eng Division Am Soc Civ Eng* 89:31–59
- Zhang Z, Ian MO, Geoff AK, William OSD (2013) Comparative study on adsorption of two cationic dyes by milled sugarcane baggase. *Ind Crops Prod* 42:41–49